A

Accession	Proteine Name	Gene Name	$\bar{X}$ iBAQ
Q96BN8	Ubiquitin thioesterase otulin	OTULIN	19.52
Q96L92	Sorting nexin-27	SNX27	18.75
O15347	High mobility group protein B3	HMGB3	16.69
Q16718*	NADH dehydrogenase [ubiquinone] 1 alpha subcomplex subunit 5	NDUFA5	15.28
Q9Y3D3*	28S ribosomal protein S16	MRPS16	15.25
O14828	Secretory carrier-associated membrane protein 3	SCAMP3	15.23
O00264*	Membrane-associated progesterone receptor component 1	PGRMC1	15.21
P40616	ADP-ribosylation factor-like protein 1	ARL1	15.19
P62495	Eukaryotic peptide chain release factor subunit 1	ETF1	15.14
P61421	V-type proton ATPase subunit d 1	ATP6V0D1	14.91
P20618	Proteasome subunit beta type-1	PSMB1	14.64
Q9HB71	Calcyclin-binding protein	CACYBP	14.58
P56556*	NADH dehydrogenase [ubiquinone] 1 alpha subcomplex subunit 6	NDUFA6	14.51
P51570	Galactokinase	GALK1	14.44
P08243	Asparagine synthetase [glutamine-hydrolyzing]	ASNS	14.39
Q9BTV4	Transmembrane protein 43	TMEM43	14.38
O15173	Membrane-associated progesterone receptor component 2	PGRMC2	14.27
P30040	Endoplasmic reticulum resident protein 29	ERP29	14.01
P00387*	NADH-cytochrome b5 reductase 3	CYB5R3	13.98
Q9Y3B4	Splicing factor 3B subunit 6	SF3B6	13.96
Q96EP0	E3 ubiquitin-protein ligase RNF31	RNF31	13.89
Q9HD45	Transmembrane 9 superfamily member 3	TM9SF3	13.64
P82664*	28S ribosomal protein S10	MRPS10	13.45
Q9UHI6	Probable ATP-dependent RNA helicase DDX20	DDX20	13.44
P50995	Annexin A11	ANXA11	13.41
O95470	Sphingosine-1-phosphate lyase 1	SGPL1	13.21
P46977	Dolichyl-diphosphooligosaccharide--protein glycosyltransferase subunit STT3A	STT3A	13.13
O00505	Importin subunit alpha-4	KPNA3	13.09
P31153	S-adenosylmethionine synthase isoform type-2	MAT2A	13.04
P28331*	NADH-ubiquinone oxidoreductase 75 kDa subunit	NDUFS1	12.93
O60841	Eukaryotic translation initiation factor 5B	EIF5B	12.91
O14734	Acyl-coenzyme A thioesterase 8	ACOT8	12.89
Q8NF37	Lysophosphatidylcholine acyltransferase 1	LPCAT1	12.83
P36507	Dual specificity mitogen-activated protein kinase kinase 2	MAP2K2	12.79
Q8IXH7	Negative elongation factor C/D	NELFCD	12.75
P82663*	28S ribosomal protein S25	MRPS25	12.66
Q01581	Hydroxymethylglutaryl-CoA synthase	HMGCS1	12.65
P48730	Casein kinase I isoform delta	CSNK1D	12.63
Q86W42	THO complex subunit 6 homolog	THOC6	12.62
Q9NRK6*	ATP-binding cassette sub-family B member 10	ABCB10	12.50
Q9H5Q4*	Dimethyladenosine transferase 2	TFB2M	12.49
P04350	Tubulin beta-4A chain	TUBB4A	12.32
Q96EY7*	Pentatricopeptide repeat domain-containing protein 3	PTCD3	12.16
Q96DV4*	39S ribosomal protein L38	MRPL38	12.15
Q9BUQ8	Probable ATP-dependent RNA helicase DDX23	DDX23	12.11
Q8N163	Cell cycle and apoptosis regulator protein 2	CCAR2	12.04
Q8WWY3	U4/U6 small nuclear ribonucleoprotein Prp31	PRPF31	11.90
P23921	Ribonucleoside-diphosphate reductase large subunit	RRM1	11.59
Q9Y6N5*	Sulfide:quinone oxidoreductase	SQRDL	11.52
Q06210	Glutamine--fructose-6-phosphate aminotransferase	GFPT1	11.49
Q05397	Focal adhesion kinase 1	PTK2	11.33
P25685	DnaJ homolog subfamily B member 1	DNAJB1	11.26
Q969Z0*	FAST kinase domain-containing protein 4	TBRG4	11.21
Q3SY69*	Mitochondrial 10-formyltetrahydrofolate dehydrogenase	ALDH1L2	11.10
O60701	UDP-glucose 6-dehydrogenase	UGDH	11.09
O94826*	Mitochondrial import receptor subunit TOM70	TOMM70A	10.89
Q13085	Acetyl-CoA carboxylase 1	ACACA	10.26
O75122	CLIP-associating protein 2	CLASP2	10.06
Q6P0Q8	Microtubule-associated serine/threonine-protein kinase 2	MAST2	9.90
Q29RF7	Sister chromatid cohesion protein PDS5 homolog A	PDS5A	9.82

B

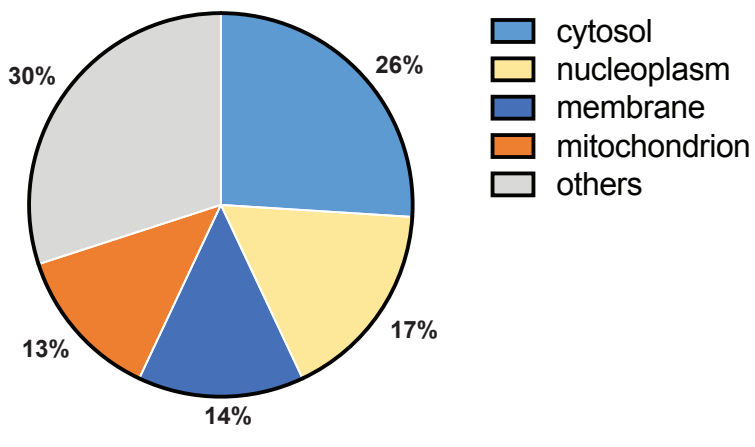

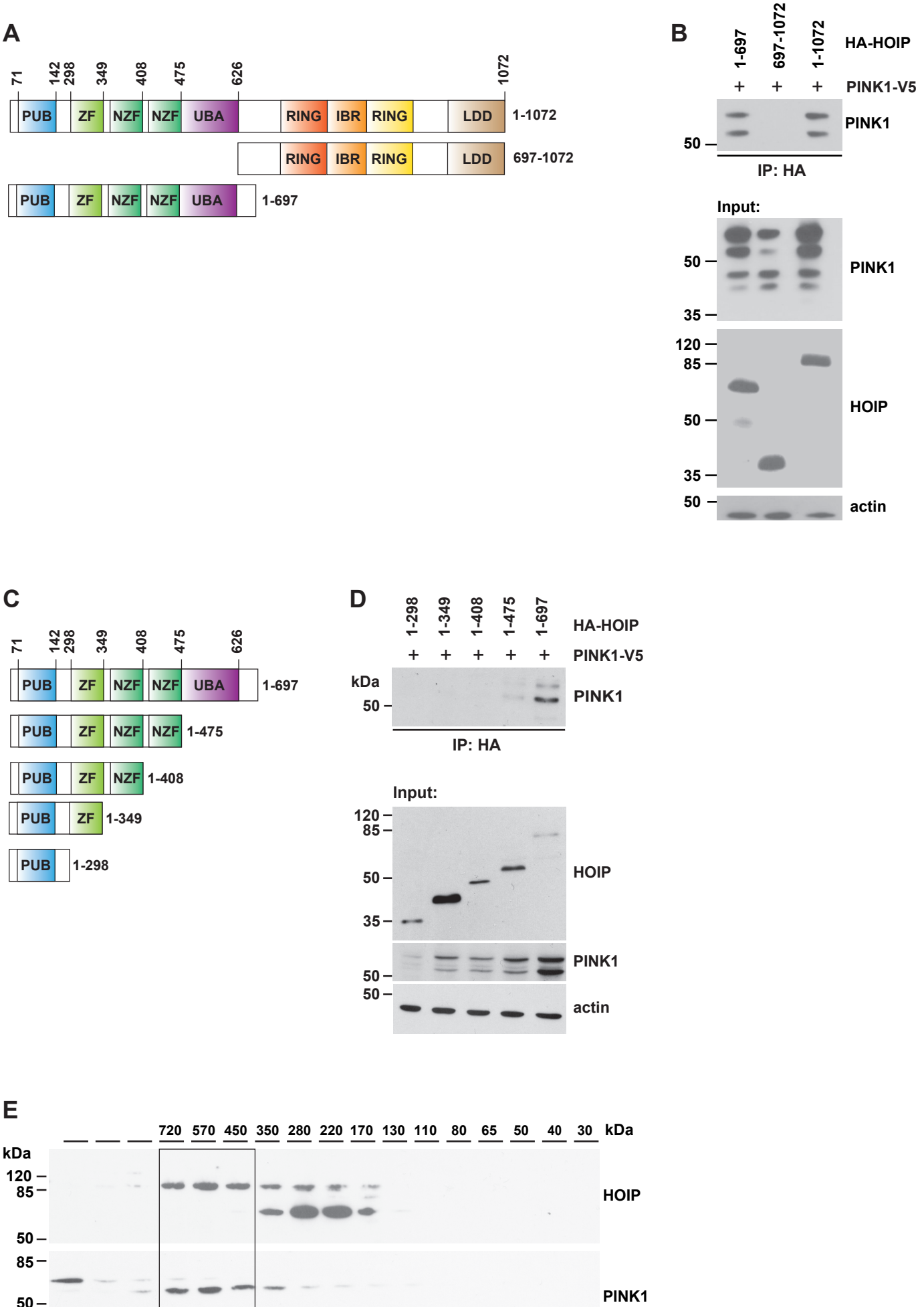
A
71
142
298
349
408
475
626
1072
PUB
ZF
NZF
NZF
UBA
RING
IBR
RING
LDD
1-1072
697-1072
1-697
B
1-697
697-1072
1-1072
HA-HOIP
PINK1-V5
PINK1
IP: HA
Input:
HOIP
actin
50
35
120
85
C
1-475
1-408
1-349
1-298
D
1-298
1-349
1-408
1-475
1-697
kDa
E
720
570
450
350
280
220
170
130
110
80
65
50
40
30

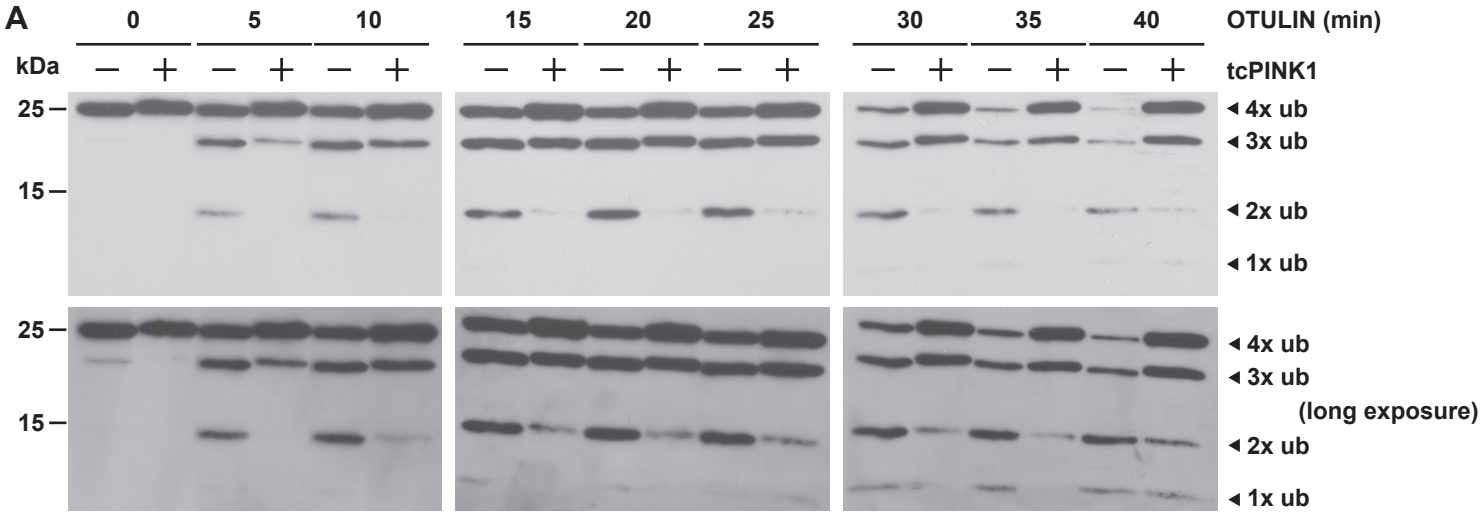
A
0
5
10
15
20
25
30
35
40
OTULIN (min)
kDa
tcPINK1
25
15
4x ub
3x ub
2x ub
1x ub
(long exposure)

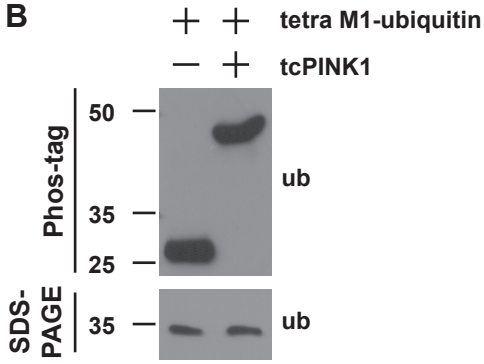
B
tetra M1-ubiquitin
tcPINK1
Phos-tag
SDS-PAGE
50
35
25
ub

Suppl. Figure 4

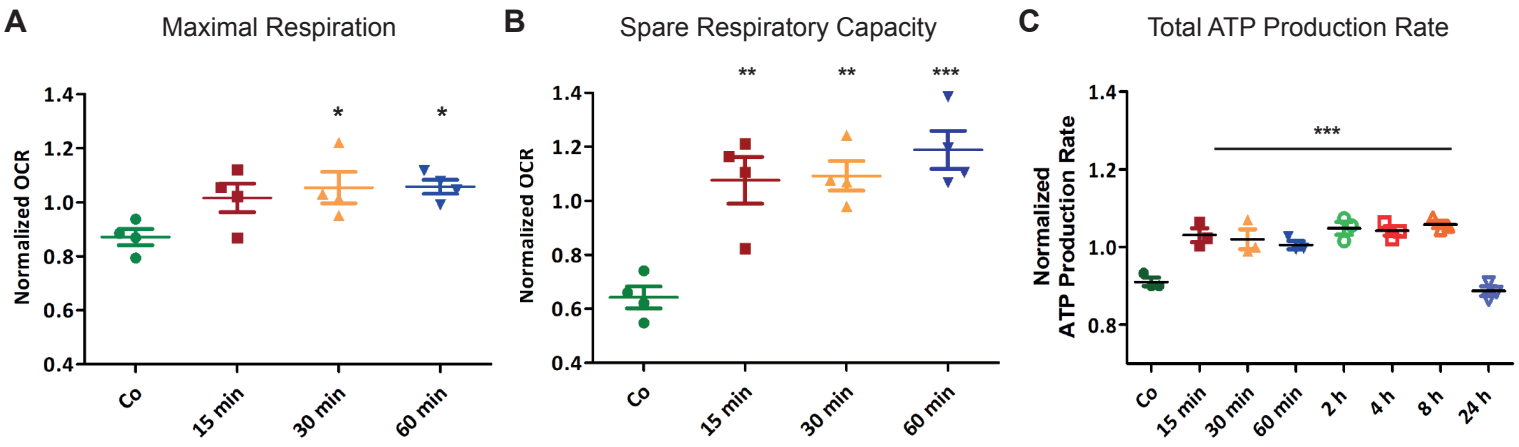

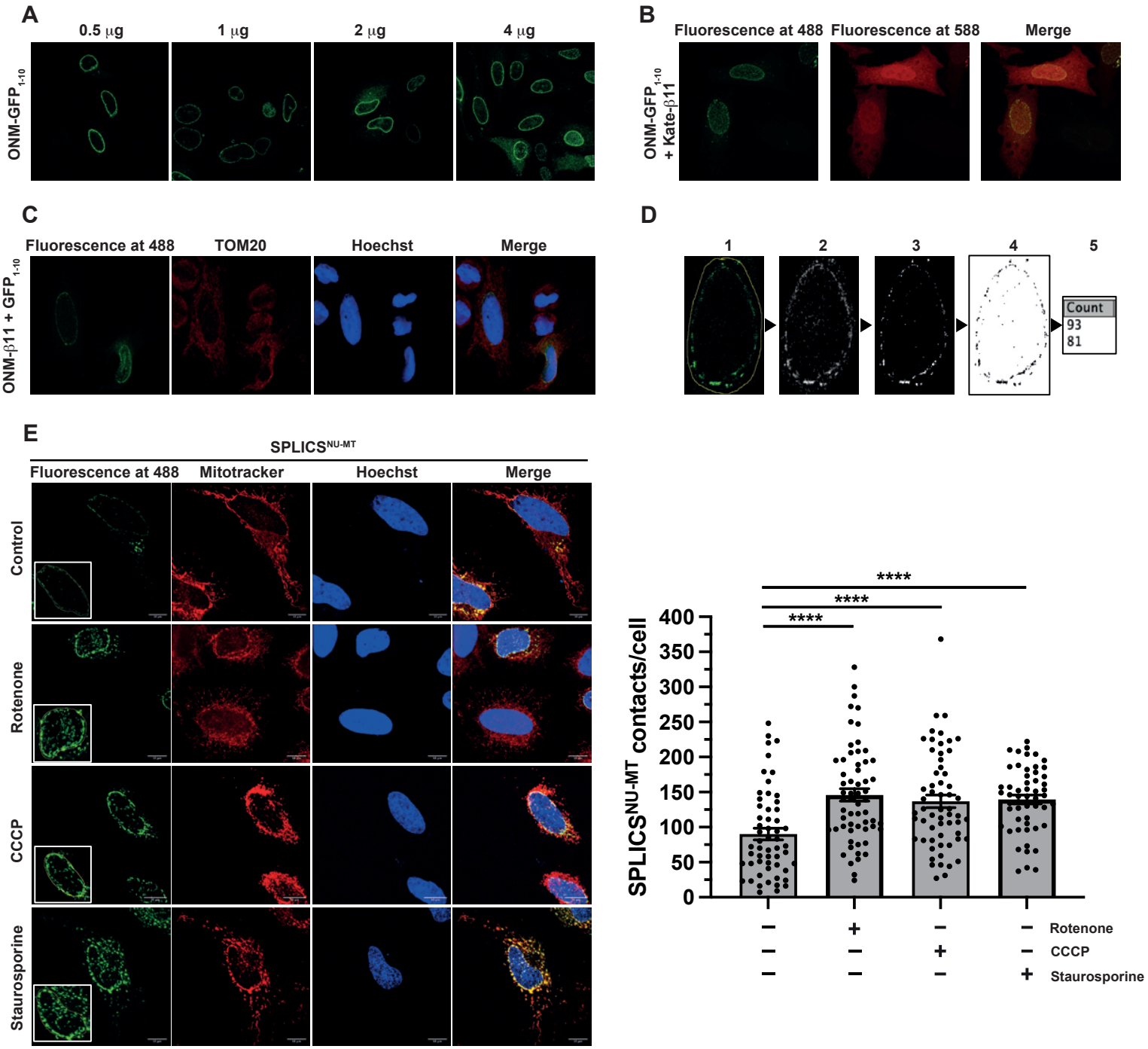
A
0.5 µg
1 µg
2 µg
4 µg
ONM-GFP1-10
B
Fluorescence at 488
Fluorescence at 588
Merge
ONM-GFP1-10 + Kate-β11
C
Fluorescence at 488
TOM20
Hoechst
Merge
ONM-β11 + GFP1-10
D
1
2
3
4
5
Count
93
81
E
SPLICSNU-MT
Fluorescence at 488
Mitotracker
Hoechst
Merge
Control
Rotenone
CCCP
Staurosporine
SPLICSNU-MT contacts/cell
400
350
300
250
200
150
100
50
0
****
****
****
Rotenone
CCCP
Staurosporine

SUPPLEMENTARY FIGURE LEGENDS

Suppl. Figure 1. Identification of OTULIN-interacting proteins by mass spectrometry

S1A. OTULIN-interacting proteins. Proteins identified by co-immunoprecipitation coupled to mass spectrometry analysis using strict filter criteria. Only proteins that were not identified in the control and that were reliably identified in both OTULIN co-immunoprecipitations by at least two unique peptides are listed according to their abundance (iBAQ-value). Mitochondria-associated proteins are marked with asterisk.

S1B. Gene Ontology cellular compartment (GOCC) characterization of OTULIN-interacting proteins. The GOCC classifications for each of the identified proteins were performed using DAVID.

Suppl. Figure 2. PINK1 interacts with the N-terminal part of HOIP including the UBA domain

S2A, C. Schematic representation of the HOIP constructs used to map the interaction between HOIP and PINK1. All constructs are equipped with an N-terminal HA-tag. PUB: peptide N- glycosidase/ubiquitin-associated domain; ZF: zinc finger domain; NZF: nuclear protein localization 4-type zinc finger domain; UBA: ubiquitin-associated domain; RING: really interesting new gene; IBR: in-between RING domain; LDD: linear ubiquitin chain determining domain.

S2B. PINK1 co-immunoprecipitates with the N-terminal part of HOIP1. HEK293T cells were transfected with V5-tagged PINK1 and the indicated HA-tagged HOIP constructs. One day after transfection cells were lysed under native conditions and subjected to immunoprecipitation using HA antibodies. Immunopurified proteins were analyzed by immunoblotting using V5 antibodies to detect PINK1.

S2D. The UBA domain enhances the interaction between HOIP and PINK1. HEK293T cells were analyzed as described in B.

S2E. PINK1 co-elutes with HOIP in cellular lysates. HEK293T cells expressing V5-tagged PINK1 were lysed, and soluble proteins were separated by size-exclusion chromatography. Fractions were collected and analyzed by immunoblotting using antibodies against HOIP and V5.

Suppl. Figure 3. PINK1 impairs OTULIN activity *in vitro*

S3A. The efficiency of OTULIN to hydrolyze M1-linked ubiquitin is decreased in the presence of PINK1. Recombinant M1-linked tetra-ubiquitin was incubated with or without recombinant *Tribolium castaneum* tcPINK1 for 48 h. Then recombinant OTULIN was added

for the indicated time. The reaction was stopped by adding Laemmli sample buffer and the samples were analyzed by immunoblotting using ubiquitin antibodies.

S3B. PINK1 phosphorylates M1-linked tetra-ubiquitin *in vitro*. M1-linked tetra-ubiquitin was incubated with or without recombinant tcPINK1 in kinase buffer for 2 days. The samples were analyzed by Phos-tag^{TM} SDS-PAGE and immunoblotting using ubiquitin antibodies.

Suppl. Figure 4. TNF influences the bioenergetic profile

S4A, B. TNF increases maximal respiration (A) and spare respiratory capacity (B). HeLa cells were treated with TNF for the indicated time and analyzed by the Agilent Seahorse XF Cell Mito Stress Test. The spare respiratory capacity is the difference between the maximal and the basal respiration.

S4C. TNF TNF increases total ATP production. HeLa cells were treated with TNF for indicated time and analyzed by the Agilent Seahorse ATP Rate Assay.

Suppl. Figure 5. Targeting, self-complementation and ability to respond to the MRR activation of the SPLICS^{NU-MT} reporters.

S5A. Assessment of the nuclear envelope localization of the ONM-targeted GFP_{1-10} fragment at different concentrations of plasmid transfected in HeLa cells. The GFP_{1-10} fragment was stained with a mouse anti-GFP primary antibody (Santa Cruz, 1:100) followed by an anti-mouse AlexaFluor 488-conjugated secondary antibody (ThermoFisher, 1:100).

S5B. Assessment of the self-complementation capability of the ONM targeted GFP_{1-10} fragment with a cytosolic mKate-tagged β11.

S5C. Nuclear envelope localization and self-complementation of the ONM-targeted β11 fragment co-transfected with an untargeted, cytosolic GFP1-10 fragment. Nuclei were stained with Hoechst33342 (ThermoFisher, 1 μg/ml).

S5D. Schematic representation of the contact quantification process using ImageJ plugin VolumeJ and custom-made macros specifically developed for the analysis: 1. a ROI is traced around the nucleus of the cell; 2. the first macro is applied, which clears all the signal outside the ROI and convolves the signal inside; 3. VolumeJ is used to generate a rendering of the convolved signal; 4. the second custom macro is applied on the first and the last frame of the rendering; 5. the contacts per each frame are quantified and the overall number of contacts per cell is calculated by averaging the two results.

S5E. Representative images and contact quantification of HeLa cells after induction of the mitochondrial retrograde response (MRR) upon treatment with rotenone (5 μM for 3 h), CCCP (10 μM for 3 h) or staurosporine (1 μM for 2 h). Mitochondria were stained with MitoTracker Red CMXRos (ThermoFisher, 100 nM) in HBSS for 30 minutes. Nuclei were stained as described in C.

Movie 1. TNF induces the movement of peripheral mitochondria towards the nucleus. SH-SY5Y cells were stained with NucSpot Live 488 and MitoView 650 for 30 min. After TNF treatment (25 ng/ml) the cells were imaged every 2 min for 30 min. Image analysis was performed by Imaris 9.8 using the Surface (nucleus) and Spot (mitochondria) algorithm. Mitochondrial distance with respect to the nuclear surface was color-coded (purple/blue = proximal; red/yellow =distal).